Chemical Engineering Journal 495 (2024) 153677

Contents lists available at ScienceDirect

Chemical Engineering Journal

journal homepage: www.elsevier.com/locate/cej

Biomethanation on demand: Continuous and intermittent hydrogen supply on biological CO_2 methanation

Aikaterini Xirostylidou [a,b], Maria Gaspari [a], Konstantinos N. Kontogiannopoulos [a], Gabriele Ghiotto [c], Laura Treu [c,*], Stefano Campanaro [c], Anastasios I. Zouboulis [b], Panagiotis G. Kougias [a,*]

[a] Soil and Water Resources Institute, Hellenic Agricultural Organisation Dimitra, Thermi-Thessaloniki 57001, Greece
[b] Laboratory of Chemical and Environmental Technology, Department of Chemistry, Aristotle University of Thessaloniki, Thessaloniki 54124, Greece
[c] Department of Biology, University of Padova, Via U. Bassi 58/b, 35121 Padua, Italy

ARTICLE INFO

Keywords:
Hydrogenotrophic methanogenesis
Trickle Bed Reactors (TBRs)
Continuous and intermittent gas supply
Biomethanation on demand
Microbial community

ABSTRACT

Achieving carbon neutrality in Europe hinges on the exploitation of renewable energy resources. Although these resources seem plentiful, critical challenges emerge from the excess energy that cannot be effectively stored or from insufficient electricity production. A promising approach to sustaining a balanced electricity network that aligns production with demand involves integrating the transformation of surplus energy into biomethane through a two-stage process. The surplus energy is utilized to produce hydrogen through water electrolysis, followed by the biological methanogenesis of hydrogen and carbon dioxide to synthesize biomethane. Investigating energy undersupply scenarios is crucial to understanding the resilience of biological processes, requiring evaluation of intermittent hydrogen supply modes and their microbial impacts. The present study focused on simulating actual demand-driven operational conditions by intermittently halting the supply of input gas, thereby inducing disruptions within the biological processes. Various sequences of consecutive starvation and regular operation phases, spanning one to five weeks, were assessed. The experimental framework was executed in two thermophilic Trickle Bed Reactors under anaerobic conditions, each utilizing distinct packing materials; specifically, activated carbon pellets and polyethylene K1 Media Raschig rings. The objective was to scrutinize the influence of these materials on the composition of the output gas, process stability and resilience of the microbial community. Remarkably, in both reactors, the biomethanation process demonstrated high adaptability, with capabilities to cease and recommence almost instantaneously, even following a five-week starvation period, effectively returning the process performance to its optimal pre-starvation state.

1. Introduction

Climate change represents an urgent and anthropogenically driven threat to Earth, attributable to the significant augmentation of greenhouse gases (GHG) beyond natural atmospheric levels. Therefore, the imperative to mitigate this phenomenon and achieve climate neutrality in Europe has arisen. Renewable energy sources play an important role in achieving this goal, and as a result, the use of wind, solar and hydroelectric power is constantly increasing. In fact, their share in total energy consumption experienced a twofold increase between 2004 and 2020 [1], contributing to the objectives of the Paris Agreement, which stipulates a reduction in greenhouse gas emissions by 55 % by the year 2050.

However, the variable and intermittent nature of these energy sources, dependent on weather and seasonal variations, poses challenges to the stability of the electricity grid. To address these challenges, in particular, during overproduction, the conversion of surplus renewable energy into gas through Power-to-Gas (PtG) technology has emerged as a viable solution [2]. This approach could involve the production of "green" hydrogen (H_2) via water electrolysis using electricity from renewable sources. Subsequently, this "green" H_2 can be utilized in conjunction with an external CO_2 source (e.g., from waste/flue gases) to produce methane (CH_4). The hydrogenation of CO_2 into CH_4 is based on the chemical reaction (Equation (1), in which one molecule of carbon dioxide reacts with four molecules of hydrogen to produce one molecule of methane (CH_4) and two molecules of liquid water [3].

* Corresponding authors.
E-mail addresses: laura.treu@unipd.it (L. Treu), p.kougias@swri.gr (P.G. Kougias).

https://doi.org/10.1016/j.cej.2024.153677
Received 19 January 2024; Received in revised form 25 April 2024; Accepted 1 July 2024
Available online 2 July 2024

$$4H_2 + CO_2 \rightarrow CH_4 + 2H_2O \quad \Delta G^o = -130.7 kJ/mol \tag{1}$$

The process can be facilitated either thermocatalytically, known as Sabatier reaction, or biologically. In the catalytic methanation, the reaction is driven by a catalyst and necessitates high temperatures ranging from 250 °C to 700 °C and pressures of up to 100 bar [4]. Contrary, the biological methanation is facilitated by specialized anaerobic hydrogenotrophic methanogens, which utilize H_2 as an electron donor to convert CO_2 into CH_4 [5]. Despite the fact that applications employing catalytic pathways exhibit greater technical maturity within the marketplace, recent advancements have seen biological methanation systems gaining traction, progressing towards an advanced stage of technological maturity [6,7]. This can be ascribed to the inherent advantages presented by biological methanation, notably its capacity to operate under milder temperature and pressure conditions [8]. As such, in November 2023, Denmark inaugurated the world's pioneering first full-scale plant for biological methanation showcasing the innovative approach to sustainable energy solutions [9].

Renewable fuels, such as methane, derived from PtG technologies, emerge as a sustainable alternative to fossil fuels. Methane could effectively substitute natural gas and integrate into the pre-existing natural gas infrastructure upon meeting the requisite purity standard, which is typically set at a minimum of 95 % methane content [10]. In this concept, methane stands as a viable and efficient fuel option in the transition towards renewable energy sources [11].

Numerous research groups which have been focusing on determining the optimal parameters for biological methanation [13,63] encountered several constraints on the volumetric production of methane. A notable challenge in this regard is the lower solubility of hydrogen in water, compared to the solubility of CO_2 (over 700 times in mesophilic (anaerobic) conditions and over 500 times in thermophilic (anaerobic) conditions) [4]. This differential solubility critically influences the efficiency of the biomethanation process.

The selection of an appropriate reactor configuration is a crucial factor in biomethanation processes. Investigations into various reactor designs have revealed that Trickle Bed Reactors (TBRs) offer superior performance in terms of biomethanation efficiency and operational cost-effectiveness [14]. The TBR configuration consists of cylindrical columns-reactors filled with packing material where the provision of H2 and CO2 is taking place. In this setup, methanogenic archaea are suspended in a process liquid, which is incrementally distributed over the packing material through a trickling mechanism. This design fosters the immobilization of microorganisms, leading to the formation of a biofilm on the surface of the packing materials. Additionally, the trickling process helps the transport of essential nutrients to the methanogens, facilitating their growth and activity [4,65]. Therefore, efficacy is attributed to the incorporation of packing materials that effectively mitigate the prevalent challenge of mass transfer limitations. Specifically, the properties of these packing materials, such as the type of material, high specific surface area, and porosity, are instrumental in enhancing the gas–liquid mass transfer processes via the development of biofilm on the surface of the packing materials [15]. This biofilm attached on the surface of packing materials is composed of a specific arrangement of immobilized cells within a matrix of extracellular polymeric substances [16].

The novelty of this study is based on the assessment of the effectiveness of different packing materials in enhancing biomethanation, under a progressive reduction of the Gas Retention Time (GRT) and with a unique focus on both continuous and intermittent hydrogen supply. This latter approach is particularly pioneering as it simulates real-world scenarios where renewable energy sources might not provide a consistent supply of green hydrogen, thus affecting the hydrogen availability for the biomethanation process. To this end, two distinct packing materials (i.e., activated carbon pellets and polyethylene K1 Media Raschig rings) were employed in two thermophilically operated, identical reactors. During the initial stage, the GRT was systematically decreased by increasing the inflow of the gas feed. Subsequently, in the second stage, the reactors were subjected to intermittent feed patterns to closely replicate real-world operational scenarios, particularly the fluctuating hydrogen supply characteristic of renewable energy sources. To the best of the authors' knowledge, this study is the first to investigate discontinuous feeding over a period of 5 weeks, marking a significant advancement in carbon capture and utilization systems for efficient and sustainable energy conversion. Concurrently, the study also focused on monitoring changes in the microbial community structure, correlating these variations with the alterations in the supply conditions of feedstock gases across both experimental stages.

2. Materials and methods

2.1. Inoculum and nutrient medium

An enriched hydrogenotrophic mixed culture obtained from thermophilic (55 °C) lab-scale biomethanation TBRs was used in the beginning of the reactors' operation as inoculum [17]. The inoculum was characterized prior to introduction into the reactors and had a pH of 7.2 ± 0.1, and a total VFA concentration of 0.013 ± 0.95 g/L. Digested sewage sludge from Thessaloniki's Municipal Wastewater Treatment Plant (MWWTP) was utilized as the nutrient source for the microbial community. Upon arrival at the laboratory, the digestate was incubated under thermophilic conditions for two months to ensure that the respective potential methane production diminished. Subsequently, it was filtered through a 2 mm sieve to eliminate large particles, preventing potential clogging issues. The pH value of the digestate was 8.6 ± 0.01 with a total VFAs content equal to 0.029 ± 1.33 g/L. The chemical composition of digestate as nutrient media and hydrogenotrophic inoculum used in the experiments are presented in Table 1. As part of the operational routine, twice weekly, a 30 mL sample was collected from the liquid storage vessel of the reactors for biochemical analyses, and an equivalent volume of digestate was introduced into the vessel.

2.2. Trickle-bed bioreactors setup

The TBRs used in this study consist primarily of a packed-bed reactor, a gas and liquid delivery system and a gas-metering system. A detailed schematic diagram of the experimental setup, alongside its associated equipment, is presented in Fig. 1. In detail, the experiment was conducted into two custom-made cylindrical-shaped TBRs of 1 L working volume. Each reactor was made of stainless-steel having a length of 55 cm and an internal diameter of 5.5 cm. The first reactor, denoted as TBR-1, was packed with activated carbon pellets (each piece had a dimension of 20 × 4 mm with a surface area 20 m^2/g, total pore volume 6 x 10^{-2} cm^3/g and micropore volume 1 x 10^{-3} cm^3/g). The second reactor, denoted as TBR-2, was filled with high-density polyethylene Raschig rings (each piece had a dimension of 10 × 10 mm with a surface area 3.3 × 10^{-3} m^2/g). The packing material was secured on a

Table 1
Chemical composition of digestate and hydrogenotrophic inoculum.

Parameter	Inoculum	Digestate
pH	7.2 ± 0.1	8.6 ± 0.1
TS, g/L	12.52 ± 0.01	31.48 ± 1.35
VS, g/L	6.95 ± 1.35	17.8 ± 0.01
TSS, g/L	11.01 ± 0.13	27.31 ± 1.14
VSS, g/L	6.41 ± 0.07	17.14 ± 0.88
TKN, g/L	0.6 ± 0.02	4.04 ± 0.18
TAN, g/L	0.25 ± 0.08	3.18 ± 0.06
Total VFA, g/L	0.013 ± 0.95	0.029 ± 1.33
Fe, ppm	22.46 ± 3.27	111.96 ± 11.19
Ni, ppm	0.15 ± 0.01	0.53 ± 0.01
Co, ppm	0.02 ± 0.01	0.09 ± 0.01
P, ppm	370.90 ± 15.22	571.96 ± 9.93

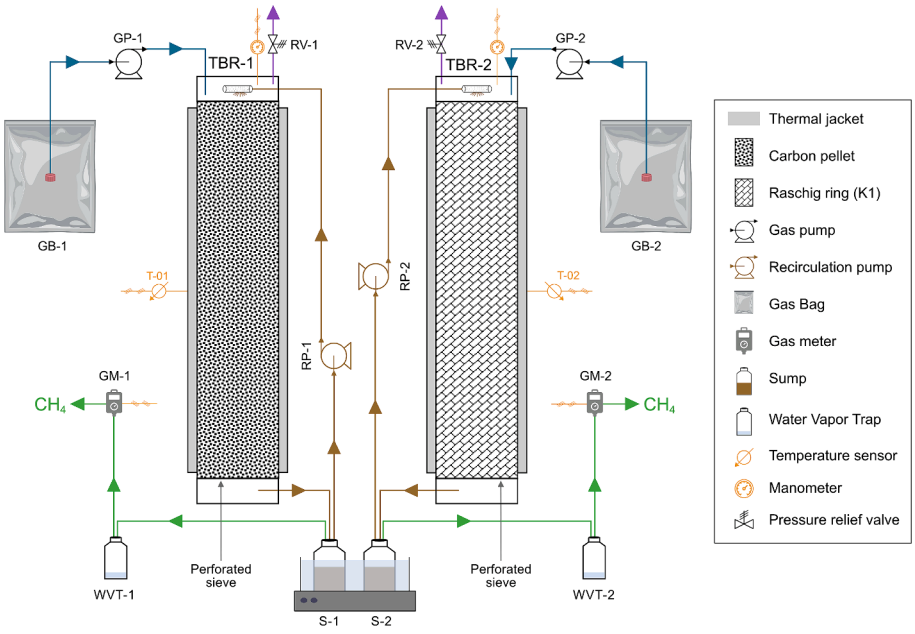

Fig. 1. Schematic diagram of the TBRs experimental units.

custom-engineered perforated sieve fabricated from stainless steel. This design facilitates the flow of both liquids and gases while preventing the packing material from being displaced. Additionally, the perforated sieve served as a barrier against the recirculation of solids, thereby mitigating the risk of reactor clogging and associated operational disruptions.

The reactors were equipped with a thermal jacket to operate at a stable thermophilic temperature (55 ± 1 °C) and with a manometer to monitor the internal pressure. Each reactor was connected to an individual liquid reservoir, namely sump (stored in a water bath to maintain stable thermophilic temperature), which contained the nutrient medium. A peristaltic pump (Sci-Q 300, Watson Marlow, United Kingdom) was used to constantly deliver the liquid from the sump to the upper part of the reactors, where it trickled onto the packing materials at a flow rate of 95 ml/min, ensuring an ample nutrient supply to the immobilized microorganisms. An artificially prepared synthetic gas mixture, consisting of 80 % H_2 and 20 % CO_2, served as the feed gas for the reactors and was continuously provided to the upper part of them through a dual-head peristaltic pump (Ismatec Reglo, Masterflex, United States). The provision of gas and liquid streams from the top of the reactors is also known as co-current, top-to-bottom strategy and according to the cited literature, this approach has emerged as the most efficient strategy for methane production, characterized by its absence of technical issues [4]. Moreover, the feeding gas-flow increased progressively over time at equal intervals in both reactors due to the dual-head pump. The gas feeding flows for each GRT are comprehensively outlined in Table 2. The output gas production of each reactor was measured daily by automated water-displacement gas meters with a 100 mL reversible cycle [18]. To remove the water, which is coproduced with methane in the biological methanation reaction, a water vapor trap was placed before each gas meter.

2.3. Operating conditions

The experimental process was divided into two distinct Stages described as follows: Stage I, both reactors operated under continuous supply conditions, while in Stage II, intermittent starvation conditions were applied. The experimental run of Stage I lasted 162 days, divided into separate phases. During each phase, the Gas Retention Time (GRT) was reduced by increasing the provision of the gas supply, i.e., the H_2 and CO_2 mixture. The transition between each phase was achieved once the composition of the output gas was stabilized above 95 % methane. The performance of the two TBRs was assessed for nine different GRTs, starting highest and ending with the lowest possible (12, 10, 8, 6, 4, 3, 2, and 1 h as well as 45 min). The process robustness was assessed by monitoring the internal pressure within each reactor, which, under optimal conditions, should remain stable. Any increase in pressure would suggest clogging or other operational issues. Throughout the 162-day operation period, the internal pressure remained consistent, fluctuating between 1.07 and 1.10 bars, indicating stable reactor performance.

In Stage II, the experimentation included five phases of starvation, each one followed by an equal time of normal operation. The starvation periods were labelled as SP1 = 1-week starvation, SP2 = 2-weeks starvation, SP3 = 3-weeks starvation, SP4 = 4-weeks starvation, and SP5 = 5-weeks starvation. Similarly, the normal operation phases were: OP1 = 1-week operation, OP2 = 2-weeks operation, OP3 = 3-weeks operation, OP4 = 4-weeks operation, and OP5 = 5-weeks operation. Fig. 2 illustrates the experimental design, depending on both the operational and starvation phases. During the regular operational periods, the bioreactors were maintained with a GRT of 1 h. In the starvation periods, the reactors did not receive any feeding gas, while the temperature conditions were consistently maintained. The impact of this starvation phase was assessed by observing the duration necessary for the bioreactors to reestablish equilibrium during the subsequent regular

Table 2
Influent CO_2 and H_2 flow rates for different Gas Retention Times (GRT).

Gas Retention Time (GRT)	12 h	10 h	8 h	6 h	4 h	3 h	2 h	1 h	45 min
Total gas input ($L \cdot L_{reactor}^{-1} \cdot h^{-1}$)	0.09	0.10	0.13	0.16	0.25	0.34	0.50	1.00	1.32
H_2 input ($L \cdot L_{reactor}^{-1} \cdot h^{-1}$)	0.07	0.08	0.10	0.13	0.20	0.27	0.40	0.80	1.06
CO_2 input ($L \cdot L_{reactor}^{-1} \cdot h^{-1}$)	0.02	0.02	0.03	0.03	0.05	0.07	0.10	0.20	0.26

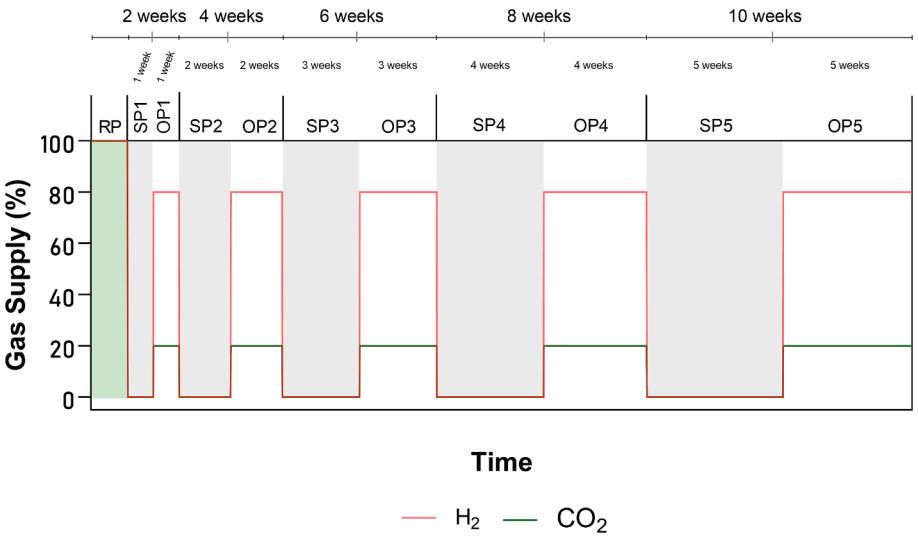

Fig. 2. Operational diagram of Stage II.

operational cycle.

2.4. Analytical methods and calculations

The gaseous phase composition was analyzed using a gas chromatography (GC-2014 Pro, Shimadzu, Japan) equipped with a thermal conductivity detector (TCD) and Porapak Q Column (1.8 m length, 1/8-inch inner diameter and film thickness 2 mm), followed by an Agilent J&W CP-Molsieve 5 Å column (1.8 m length, 1/8-inch inner diameter and film thickness 2 mm) with helium as the carrier gas and the flow rate is set at 20 mL/min. The temperature for both the column and the detector was set at 100 °C. The concentration of the output gas was determined by applying appropriate calibration curves, and the data acquired was analyzed using LabSolutions Software v5.106.

Liquid samples were collected twice per week for the analysis of pH and volatile fatty acids (VFAs). The pH was monitored with a pH meter (HI2020 EDGE, HANNA Instruments, USA) equipped with a suitable electrode. The pH of the reactors was measured before the measurements of Volatile Fatty Acids and the introduction of nutrient media. Gas chromatography (GC-2010 Pro, Shimadzu, Japan) was used for the determination of the concentration of VFAs following the protocol of Anagnostopoulou et al. [19]. The chromatograph was equipped with a flame ionization detector (FID) and an Agilent J & W Capillary Column (30 m length, 0.5 mm inner diameter, film thickness 1.0 μm) with helium, hydrogen, and synthetic air as carrier gases. Employing the appropriate calibration curves, the quantification of VFAs was evaluated, and the data were processed using LabSolutions Software version 5.106.

The efficiency of H_2 utilization (η_{H_2}, %) was determined by Eq. (2):

$$\eta_{H_2} = \frac{H_{2utilized}}{H_{2in}} \times 100 \quad (2)$$

where, $H_{2utilized}$ (L· $L_{reactor}^{-1}$ · day^{-1}) is the H_2 utilization rate and H_{2in} (L· $L_{reactor}^{-1}$ · day^{-1}) represents H_2 flow rate fed to the reactors and was calculated by Eq. (3):

$$H_{2utilized} = H_{2in} - H_{2out} \quad (3)$$

where, H_{2out} (L· $L_{reactor}^{-1}$ · day^{-1}) represents H_2 flow rate in the effluent gas.

The CO_2 conversion efficiency (η_{CO_2}, %) was calculated similarly, which also corresponds to the performance of the TBRs since the overall yield of the process is quantified based on the capture and utilization rate of CO_2.

2.5. Microbial community analysis

Genomic samples were collected from the liquid phase of the reactors on the last day of each operation change, which was either the day prior to the GRT reductions (Stage I) or the day before the starts/stops of H_2/CO_2 supply (Stage II). DNA extraction was carried out employing the DNeasy® PowerSoil® Kit (QIAGEN, Hilden, Germany), following the manufacturer's recommended procedure. The library was prepared using the Nextera DNA Flex Library Prep Kit (Illumina Inc. in San Diego, CA.) and sequencing was conducted on an Illumina NextSeq 500 platform (Illumina Inc. in San Diego, CA.). The sequencing process was performed at the CRIBI Biotechnology Center sequencing facility (University of Padova, Italy).

The reads underwent filtering using Trimmomatic v0.39 [20] to eliminate adapters and low-quality bases and were screened for contamination utilizing the BBDuck (v38.93) tool [21]. The filtered reads were subsequently aligned against the MetaPhlAn v4 database [22], employing the short-read aligner bowtie2 v2.5.1 [23] with the following parameters: −-sam-no-hd, −-sam-no-sq, −–no-unal, −-very-sensitive. The resulting SAM files were processed through MetaPhlAn v4 to extract microbial composition profiles of the examined community. The software was executed using the −-tax_lev g parameter, ensuring the acquisition of taxonomic assignments at the genus level, which is both distinct and unambiguous. To merge the output data from multiple samples into a unified table featuring the relative normalized abundances for each identified genus per sample, the script merge_metaphlan_tables.py was applied. Raw sequences are available in the NCBI database (SRA) that can be accessed under the BioProject ID PRJNA1049757.

3. Results and discussion

3.1. Continuous hydrogen and carbon dioxide supply

3.1.1. Process performance and efficiency of Trickle Bed reactors

The assessment of TBRs focused primarily on analyzing the composition of the output gas. The performance of the reactors under continuous hydrogen supply during the initial stage is presented in Fig. 3. With a GRT of 12 h, methane concentration in the output gas of both reactors achieved the requirement of 95 % content in just one-day post-initiation and maintained this level throughout the phase. This efficiency is attributed to the utilization of an active inoculum from prior laboratory experiments, which expedited microbial acclimatization. According to Ebrahimian et al. [65], the high biomethanation performance of TBRs is

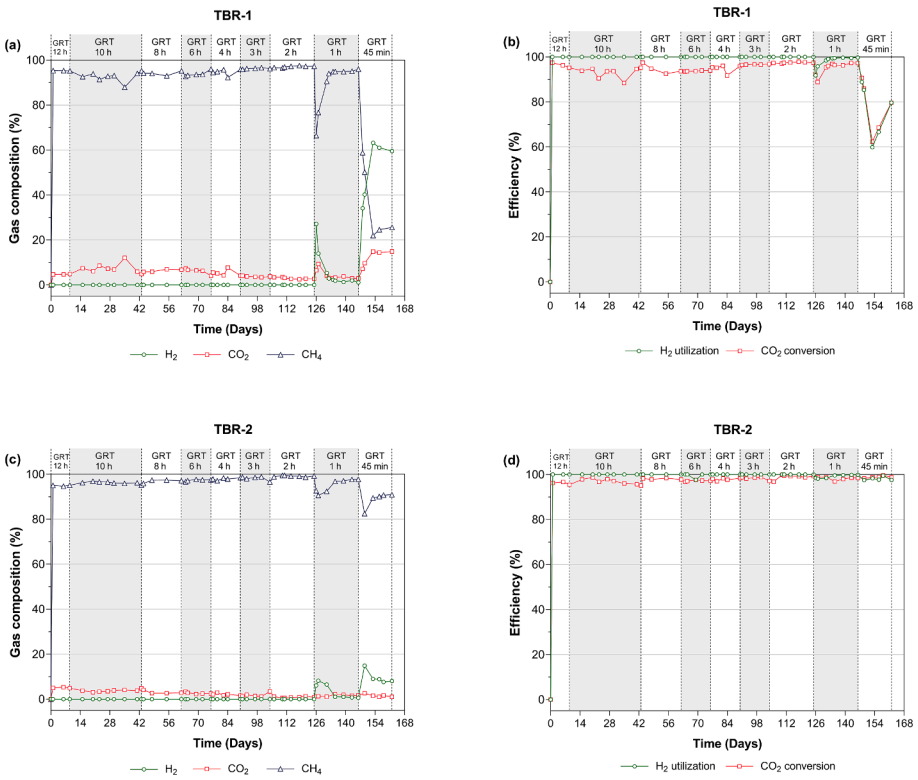

Fig. 3. Output gas composition, H_2 utilization efficiency (η_{H_2}) and CO_2 conversion efficiency (η_{CO_2}) during Stage I for TBR-1 filled with activated carbon pellets (a and b); and TBR-2 filled with K1 Media Rashig rings (c and d). Phases are separated by dashed lines.

a result of the formation of adequate biofilm on the surface of the packing materials. This biofilm comprises specific microbial entities, notably hydrogenotrophic methanogens, which play a pivotal role in the biomethanation process. The duration for biofilm formation by these microorganisms varies; however, it has been observed that many can establish biofilms rapidly, typically within 48 h [24].

The performance evaluation of TBR-1 during the reduction of GRT from 12 to 2 h revealed notable instantaneous efficiency drops at GRT 10 and 4 h. However, these incidents did not remarkably influence the reactor operation as the H_2 utilisation efficiency exceeded 95 %. The only Phase that required an extended duration to attain stable methane production was at GRT 10 h. This phenomenon is attributable to biofilm development on the packing material, which, over the operational period, exceeded the material's tolerance limit. As indicated in the study by Feickert Fenske et al. [4], an excessively thick biofilm impedes gas transfer, resulting in methanogen deactivation and necessitating biofilm redevelopment. In the case of the minor performance reduction at GRT 4 h, there is a correlation with a marginal increase in total VFAs. Nonetheless, the reactor demonstrated resilience by restoring its efficiency within five days in both instances, ultimately achieving a CH_4 concentration of 97 % at the end of the GRT 2 h phase.

In TBR-2, methane production exhibited a consistent increase of approximately 1 % with each reduction in GRT, achieving a peak methane content of 99 % at 2 h GRT, as illustrated in Fig. 3c and over 98 % of H_2 utilization efficiency (Fig. 3d). Notably, both reactors reached maximal methane production at this GRT duration. TBR-2 maintained stable functionality with a methane content of 99 %, meeting the criteria for gas grid injection (>95 %) and superior CO_2 conversion efficiency. The only difference lies in the longer adjustment time of the TBR-1, which is probably attributed to the interaction between its distinct packing material and biofilm development. Transitioning to GRT 1 h, both reactors presented fluctuations from the first day in methane output. TBR-1 experienced a more pronounced impact, with methane concentration in the output gas dropping to 66.4 %, leading to elevated levels of unutilized hydrogen and carbon dioxide. As depicted in Fig. 3a, TBR-1 necessitated eight days to restore methane concentration above 95 %, aligning with similar findings from Ghofrani-Isfahani et al. [25] that indicate reduced performance during the first several days of the reactor operation at lower GRTs. Conversely, TBR-2 demonstrated comparatively milder fluctuations and a more consistent operational profile, achieving a methane efficiency of 97 %.

During the reduction of GRT to 45 min, distinct efficiencies were observed in both reactors. TBR-1 experienced a consistent decline in methane concentration throughout the phase, reaching a final value of 25.6 %. This decline in TBR-1′s performance is potentially due to the washout of microorganisms from the biofilm, due to elevated feed rate [26]. In contrast, TBR-2 exhibited a temporary decrease in methane output, with the concentration dropping to 82.48 % during initial days but beginning to stabilize at 90 % by the seventh day of the GRT 45 min phase. From the reduction in methane efficiency, it is apparent that the H_2 and CO_2 undergo partial conversion to methane, a process which predicates two primary outcomes for the fate of these injected gases. Firstly, unreacted gases may exit the reactor, a scenario quantifiable by analyzing the gas composition post-exit, and secondly, they may undergo further biochemical conversion into acetic acid through homoacetogenic pathway as an alternative H_2 sink within the reactor environment. The metrics pertaining to ultimate H_2 utilization and CO_2 conversion efficiency, as illustrated in Fig. 3d, substantiate the comprehensive utilization of both gases for the biosynthesis of acetic acid within the reactor chamber. This conclusion, as it will be also elaborated upon the subsequent section, is further supported by the VFA analytical data, with Fig. 4b elucidating a pronounced augmentation in acetic acid concentration. Such an observation aligns with earlier studies [12,27] showing that at higher gas flow rates, a percentage of the substrate is consumed by homoacetogens for acetic acid production.

The comparative analysis of biomethanation efficiency in the two reactors indicated that TBR-2 demonstrated a more uniform methane production throughout the experimental duration. This consistency

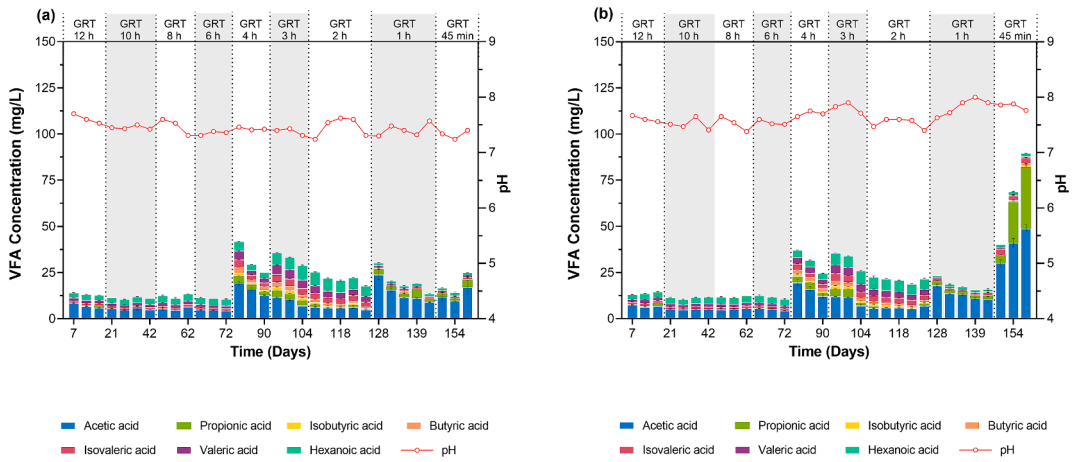

Fig. 4. Monitoring pH and VFAs concentration in (a) TBR-1 (activated carbon pellets); and (b) TBR-2 (K1 Media Raschig rings).

underscores the efficacy of Raschig rings in facilitating the development of a well-organized microbial biofilm, notwithstanding their comparatively limited specific surface area. This observed performance can potentially be attributed to the properties of commercial inorganic packing materials, which typically possess a smoother surface texture, alongside a distinct shape and structural integrity, thereby creating favorable conditions for microbial colonization and activity [28].

3.1.2. Volatile fatty acids concentration and pH values of the Trickle Bed reactors

Fig. 4 presents the VFAs concentrations and pH measurements for both reactors across the entire experimentation period. Excluding the GRT 45 min phase, no significant differences between the two reactors were observed. Specifically, the total VFAs concentrations remained stable, averaging 19.3 ± 0.5 mg/L for TBR-1 and 18.8 ± 0.9 mg/L for TBR-2 during all phases except at GRT 45 min. Comparing the values of total VFAs with previous studies [29,30], these VFA levels were notably lower. A possible explanation lies in the chemical composition of the hydrogenotrophic inoculum and the degassed digestate used in this study, which were comparatively lower than those documented in the literature. Additionally, the average pH values maintained stable throughout the whole experimental duration at 7.5 for TBR-1 and 7.7 for TBR-2, aligning with the optimal range of 7.0 and 8.0, as reported in the study by Weiland [31].

On day 79, coinciding with the reduction of GRT from 6 to 4 h, both TBRs experienced a notable increase in VFAs concentrations for the first time, escalating from 10.8 to 42 mg/L in TBR-1 and from 10.7 to 37.2 mg/L in TBR-2. This elevation in VFA levels signifies an impact on the microbial ecosystem within the reactors. However, this increment did not significantly impede reactor stability, as evidenced by the uninterrupted methane production and purity, as well as the consistent pH levels. In addition, both reactors exhibited stable VFA concentration levels during GRT 3 h, followed by a modest reduction in concentration in GRT 2 and 1 h. During the GRT 1 h, however, a redistribution of the percentages of the individual VFAs was observed, with acetic acid becoming predominant in both reactors. This finding can be associated with the results of the microbial analysis showing a slight increase in the abundance of microorganisms that are able to act as H_2 sinks and produce acetic acid. An interesting observation, nonetheless, is the low level of total VFAs, which contrasted with the methane yield of TBR-1, where a reduction in methane output was observed despite low VFA levels. Consistent with previous studies, the fluctuations in performance could be attributed to the high rates of liquid recirculation, which potentially compromised the structure and function of the hydrogenotrophic methanogens and led to the washout of biofilm from the surface of the packing materials [32,33].

In the final phase of the GRT 45 min, a significant difference in the concentration of total VFAs was observed between the two reactors, with average values being 18.7 ± 3.5 mg/L in TBR-1 and 66.3 ± 2.3 mg/L in TBR-2. TBR-1 follows a similar trend to the previous GRT reductions, experiencing a slight increase in VFA concentration and a sharp decrease in methane content in the output gas. This trend is likely attributable to biofilm damage resulting from the intensified input gas rate, hindering effective biofilm regeneration in the reactor. Conversely, TBR-2 demonstrated a more stable methane production profile during the GRT 45 min phase. The increment in total VFAs, peaking at 90 mg/L on the last day of the experiment, induced relatively minor disruptions in methane output (approx. 7 %). This decrease could be attributed to the increased tolerance of homoacetogenic bacteria to elevated partial H_2 pressures as a result of the low GRT [34].

3.1.3. Microbial community analysis of Trickle Bed reactors

In order to explore the microbial rearrangements resulting from the GRT reductions, genomic samples were collected from the liquid phase of the two reactors on the last day of each GRT. The microbial members were grouped based on their Genus level (or, when not feasible, at a higher taxonomic level) and the main results are presented in Fig. 5. It should be noted that only clusters with a relative abundance of at least 0.1 % at a one-time point were considered for further investigation. Taxonomic classification analysis revealed that, despite originating from the same inoculum, the microbial community structure of the two reactors diverged over time, with TBR-2 presenting a higher abundance of hydrogenotrophic methanogen (*Methanothermobacter* spp.) compared to TBR-1. This distinctive performance observed between the two reactors may be primarily attributed to the variance in their filling materials. This hypothesis aligns with findings from a prior study by Daglioglu et al. [35], where the use of different packing materials resulted in the formation of distinct microbial communities. In these communities, the dominance of hydrogenotrophic methanogens was expected since these are the sole contributors to methane production through the reduction of CO_2 with the utilization of H_2.

Analyzing the micro-communities of reactors, in the TBR-1 the percentage of *Methanothermobacter* spp. initiated with a lower rate (50 %) as compared to TBR-2 (77.7 %). Notably, this disparity did not have an impact on methane production, as both reactors achieved a rate of 95 % CO_2 conversion while maintaining low concentrations of total VFAs. According to the literature, this genus includes species that are thermophilic and hydrogenotrophic and have been recognized for their effectiveness in cyclic carbon economies and contemporary applications in gas-to-energy conversion technologies [36,37]. Moreover, their high abundance is in agreement with previous studies that identified members of this genus as dominant in thermophilic biogas upgrading systems

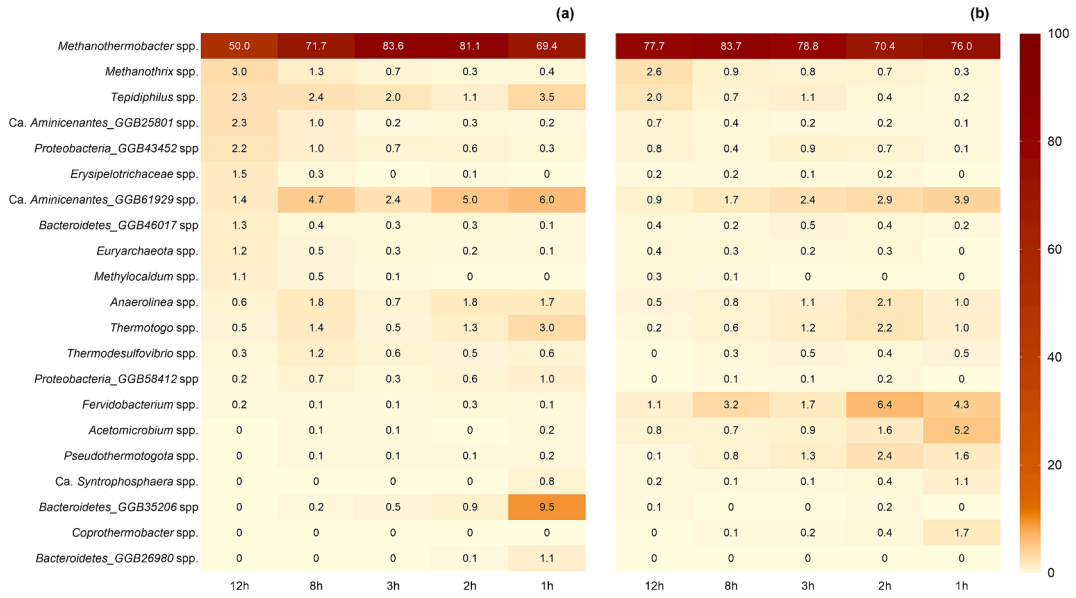

Fig. 5. Cluster heatmap of relative abundances between the MAGs of different samples in the liquid media of (a) TBR-1 (activated carbon pellets); and (b) TBR-2 (K1 Media Raschig rings) during Stage I. The colour scale is shown on the right of the heatmap, which varies from low abundance (light yellow) to high abundance (deep red).

[41,64]. Additionally, a marked rise in *Bacteroidetes*_GGB35206 during the 1-hour GRT phase in TBR-1 was noteworthy. Studies indicate that the phylum *Bacteroidetes* is renowned for its role in acetic acid production and accumulation within bacterial communities, a phenomenon also detected in this study, where acetic acid prominently constituted the total VFAs [39]. Concurrently, in TBR-1, three more bacterial genera occurred in higher abundance than the others, specifically *Tepidiphilus, Thermotoga* and Candidatus *Aminicenantes*, although remaining at low levels compared to the dominant hydrogenotrophic methanogen. Particularly Ca. *Aminicenantes_GGB43452,* exhibited an upward trend as the GRT decreased. According to the existing literature, microorganisms belonging to this phylum can convert carbon sources to volatile fatty acids [40].

In TBR-2, *Methanothermobacter* spp. predominantly constitute 70–80 % of the microbial community, playing a crucial role in methane generation from substrates. Consistent behaviour was observed for the *Methanothrix* spp. within both reactors, with a noted decrease in their abundance correlating to a marginal rise in acetic acid concentration. This pattern aligns with Jetten et al. [41], who reported the prevalence of *Methanothrix* spp. in low acetate environments. The rise in the populations of microorganisms belonging to the genera *Fervidobacteria, Acetomicrobium* and *Pseudothermotoga* in low GRTs signifies a notable differentiation between the two reactors. The increasing abundance of *Fervidobacterium* spp. could represent an indication of the preference of material type, in this instance the Raschig rings, which are probably detached from the produced biofilm and are part of the liquid phase of the reactor, a finding also observed in a previous study [17]. Moreover, *Acetomicrobium* spp. known for acetic acid production in anaerobic bioreactors, exhibited a growth of 5.2 % at the GRT-1 h phase. The increased abundance of *Acetomicrobium* spp. in CO_2 hydrogenation reactors is in accordance with previous studies, concluding that their role in such ecosystems is attributed to supporting the growth and metabolism of *Methanothermobacter* spp. [22,62]. Furthermore, *Pseudothermotoga* a bacterium known as a thermophilic fermentative anaerobic H_2 producer, increased to 1.6 %.

3.2. Biomethanation on demand by intermittent hydrogen and carbon dioxide supply

3.2.1. Process performance and efficiency before and after starvation

The understanding of how the on-demand biomethanation process responds to intermittent H_2 supply is crucial, especially considering the frequent changes in electrical grids in real-world scenarios. This study aimed to monitor the reactors' performance during starvation periods, defined as phases without influent feedstock, and to analyze the impact on microbial communities. Upon the completion of Stage I, the GRT of the reactors was adjusted to 1 h and maintained until a stable operation with a minimum methane efficiency of 95 % was achieved. Once this threshold was obtained, Stage II of the experimental process was initiated. Fig. 6 illustrates the performance of TBR-1 and TBR-2 under intermittent hydrogen and carbon dioxide supply across all operational phases. Assessment of the TBRs performance was carried out in the same way as in the previous Stage, in terms of the output gas composition.

In the initial Starvation Period (SP1) of both reactors, methane levels decreased not lower than 18 %, depicting that residual intermediates remained within the reactors, allowing the bacterial representatives of the community to metabolize and convert them into methanogenic substrates. This indicates that a one-week starvation period was insufficient for complete substrate depletion, contrasting with Logroño et al. [42], who reported substrate exhaustion in 24 h. During the subsequent Operational Phase 1 (OP1), TBR-1 demonstrated remarkable resilience and efficiency, achieving 97 % methane in the output gas within a day of resuming operation, and stabilizing at approximately 98 % methane concentration, as depicted in Fig. 6a. This efficiency highlights the robustness of the microbial community in TBR-1, capable of sustaining biological conversion after a week of starvation, aligning with the findings of study Khesali Aghtaei et al. [43]. Conversely, TBR-2 displayed a slower recovery, initially producing 69 % methane, which gradually increased to 96 % by the end of OP1's first week, as illustrated in Fig. 6c. This pattern indicates that the microbial community in TBR-2 required additional time to recover from the feedstock interruption and attain optimal biomethane production efficiency.

In the second Starvation Phase (SP2), extending the no-feed period to two weeks, the performance metrics of both reactors mirrored those observed in SP1. TBR-1 demonstrated remarkable adaptability, rapidly reverting to stable operations upon resuming the feed, while TBR-2

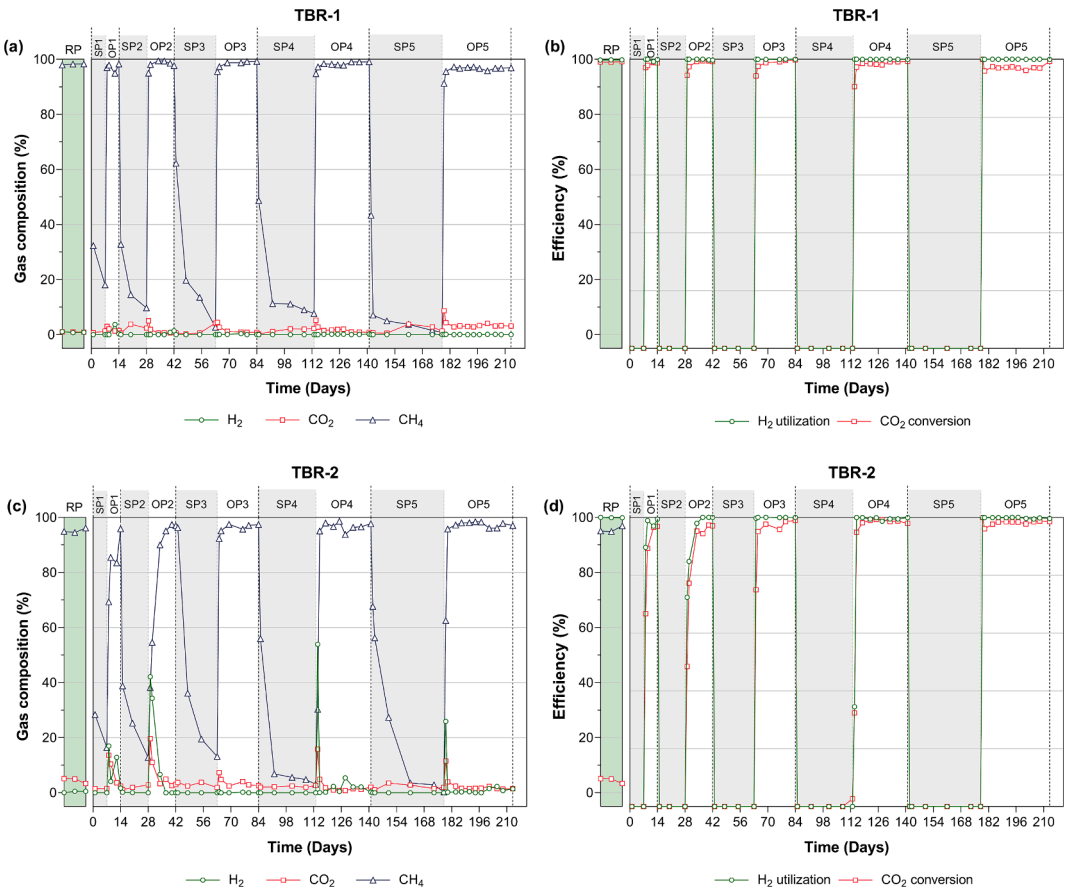

Fig. 6. Output gas composition, H_2 utilization efficiency (η_{H_2}) and CO_2 conversion efficiency (η_{CO_2}) during Recovery Period-RP (green colour); Starvation Periods-SP (grey colour); and normal Operation Phases –OP (white colour) of Stage II for TBR-1 filled with activated carbon pellets (a and b); and TBR-2 filled with K1 Media Rashig rings (c and d).

necessitated eight days to achieve the 95 % methane concentration threshold. The performance peaked during the final day of the two-week operational period, with TBR-1 attaining a methane output of 98 % and TBR-2 reaching 97 %.

Subsequently, in a phase involving three weeks of feed deprivation (SP3) followed by an equal duration of continuous operation (OP3), both reactors efficiently reached methane outputs exceeding 95 % in a relatively short time. Notably, TBR-2 exhibited a significantly improved performance compared to the other two periods in terms of the time required to attain a methane content exceeding 95 % (Fig. 6c). This enhancement in biomethanation efficiency during the third phase is indicative of the development of sufficient biofilm consisting of specialized microorganisms for biomethanation.

Upon completion of the second experimental Stage, a consistent pattern emerged in the performance of both TBR-1 and TBR-2 across the final two periods. Methane production was consistently high in the feed phases (OP4, and OP5) reaching 97 % in both reactors on the last day of phase 5. The quick adaptation of the microbial community most likely indicates the rapid reactivation of the methanogenic population regardless of the number of weeks of starvation. Notably, TBR-1 exhibited superior efficiency from the outset of each phase, maintaining methane rates above 91 % from day one. In contrast, TBR-2 typically necessitated up to three days to regain optimal performance levels. The enhanced efficiency of TBR-1 can be ascribed to its higher contact surface area, attributable to the larger specific surface area of the activated carbon used. This feature promotes a more effective liquid–gas mass transfer of H_2 to the biofilm allowing more adequate formation of biofilm [44,45].

A limited number of investigations have been carried out studying the process of methanogenesis during intermittent CO_2 and H_2 feeding. This study is pioneer in introducing a novel perspective to the field by focusing on an extended period of equal starvation and operation phases, surpassing one month, a duration not reported in the existing literature. Previous studies in this area typically documented short-term responses, ranging from a few minutes to several hours, indicating a rapid initiation of biomethanation after a short period of time and, therefore the robustness of the microbial community [46]. Longer periods of starvation, extending up to four weeks, required a longer adaptation time for reactors to regain optimal performance, sometimes taking as long as a week. In our study, TBR-1 demonstrated a more stable performance in terms of recovery, while TBR-2 required additional time, varying from a few days to a week, for performance restoration. This finding is consistent with a previous study from Braga Nan et al. [47] which suggest that the choice of packing material in combination with the biofilm formation has an impact on the overall process efficiency.

3.2.2. Volatile fatty acids concentration and pH values of the Trickle Bed reactors under intermittent H_2 and CO_2 provision

Fig. 7 illustrates the data for VFA concentrations and the pH values for both reactors during Stage II of the experiment. The pH in each reactor exhibited comparable trends, averaging around 8.5. Specifically, TBR-1 and TBR-2 maintained pH levels within the ranges of 8.1 to 8.9 and 8.2 to 8.9, respectively, throughout the experimental duration. As mentioned, the ideal pH range for methanogenesis is typically between 6.0 and 8.5 [48]. Nevertheless, ex-situ methanogenesis also takes place in a more alkaline environment as a consequence of external H_2 supply and CO_2 uptake. This finding is supported by several investigations, including a study by Ashraf et al. (2020) [49], who reported that TBR

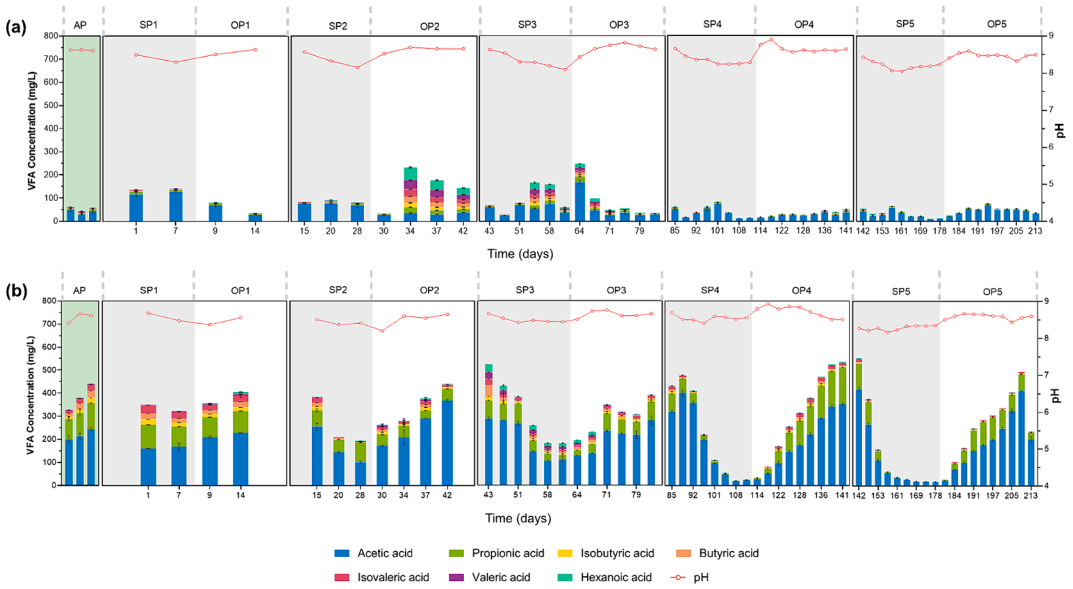

Fig. 7. Monitoring pH and VFAs concentration during Recovery Period-RP (green colour); Starvation Periods-SP (grey colour); and normal Operation Phases-OP (white colour) of Stage II for (a) TBR-1 (activated carbon pellets) and (b) TBR-2 (K1 Media Raschig rings).

remained unaffected even with pH approaching 9.0, indicating the tolerance of the microbial community to more alkaline conditions. Similarly, Dupnock & Deshusses [50] observed an increase in methane percentage at pH 9.0. An alternative study stated that pH values exceeding 9.0 are conducive to hydrogenotrophic methanogenesis over acetoclastic [51].

As depicted in Fig. 7a, TBR-1 exhibited notably lower total VFA levels, maintaining consistent concentrations across both normal operation and starvation periods. Within the VFA profile, acetic acid predominated over other VFAs, aligning with findings from previous studies [52,53]. The average concentration of acetic acid in TBR-1 was 44.3 ± 2.5 mg/L, peaking at 116.7 mg/L on the first day of the operation phase, which is relatively lower compared to ranges reported in other studies [54]. Relatively elevated concentrations of the individual VFAs were observed during OP2, SP3 and OP3. Nevertheless, this increase did not impact the methanogenesis process, as the methane output consistently exceeded 95 %. Subsequently, the stability of VFAs content suggests that the microbial community of TBR-1 was not affected by the intermittent feeding, indicative of an efficient biofilm formation on the packing material (activated carbon) and the formation of a robust community of microorganisms. This outcome suggests that the properties of activated carbon, particularly its high specific surface area, are helpful during intermittent hydrogen supply, enhancing the biomethanation process [55].

In TBR-2, a distinctive microbial structure was evident, leading to elevated levels of VFAs, which induced a slow adaptation during shifts of gas feeding conditions. The highest value of total VFAs occurred on the first day of the experiment, with a value of 351.7 mg/L. This peak correlated with a significant increase of VFA to 440.3 mg/L during the last phase of the preceding experiment and the adjustment to GRT 1 h. Nonetheless, previous study has shown that values up to 1000 mg/L indicate a well-functioning process [56]. As illustrated in Fig. 7, a consistent pattern is observed throughout the whole experimental period. This pattern involved a continuous increase in VFA concentration during feedstock supply periods, followed by a decline in concentration during the starvation periods. Notably, the starvation periods in Phases 4 and 5 resulted in a near-elimination of VFA concentrations. Acetic acid and propionic acid were the predominant VFAs, aligning with findings from previous studies [32,65]. The production of propionic acid in a microbiological community is induced by stress conditions; which in this specific study, represent the intermittent supply. Finally, the remaining individual VFAs constituted a minor fraction of the total VFA concentration in TBR-2.

3.2.3. Fluctuations in microbial community composition during the start and stop feeding periods

With the aim of elucidating the changes in microbial community structure during the starvation and normal operation periods, genomic samples were collected from the liquid phase of each reactor on the final day of each period. Fig. 8 shows, using heatmap configuration, the grouped microbial members detected in the liquid media, following the same strategy as in Stage I. Overall, the microbial community was clearly affected by the periods of starvation to which they were subjected, showing also discernible differences between the two reactors. Specifically, TBR-1 continued to be dominated by the *Methanothermobacter* genus for most of Stage II, while TBR-2 exhibited a redistribution of the percentages of hydrogenotrophic methanogens (*Methanothermobacter* spp.) and bacteria compared to the previous Stage.

During the recovery period, prior to the commencement of Stage II, both reactors exhibited marked variations in their microbial community structure. This observation is intriguing, as the community composition of TBR-2 showed a rapid change during the transition of GRT from 45 min to 1 h (start of Stage II), in contrast to the microbial community of TBR-1, which was slightly affected. Based on taxonomic analysis, the archaea of both microbial communities consist of three genera: *Methanothermobacter, Methanothrix* and *Methanosarsina.* The hydrogenotrophic *Methanothermobacter* was the dominant genus in TBR-1, accounting for up to 88.2 % of the community. This aligns with established research, in which it has consistently emerged as the dominant methanogen, particularly thriving in both liquid phase and biofilm environments at thermophilic temperatures [12,57]. Therefore, the rapid recovery of high methane efficiency after all starvation periods in the first reactor can be attributed to its significant presence at abundance ranging from 43 % to 86 %. In contrast to the second reactor, which exhibited a lower relative abundance of *Methanothermobacter* (<40 %) with slower recovery during all phases of normal operation.

The dominant Phyla in the bacterial community were *Firmicutes*, *Tenericutes*, *Pseudomonodota*, and *Coprothermobacterota*. An interesting pattern regarding their presence in the communities of the two reactors was observed. Specifically, both reactors were dominated by *Methanothermobacter* spp. during periods of normal operation, while bacterial

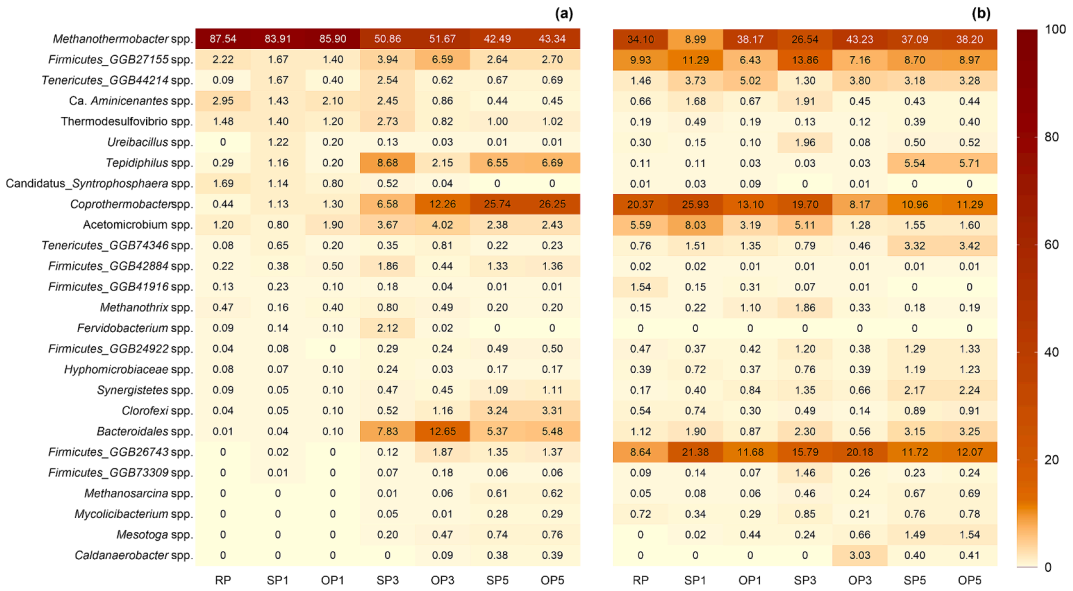

Fig. 8. Cluster heatmap of relative abundances between the MAGs of different samples in the liquid media of (a) TBR-1 (activated carbon pellets); and (b) TBR-2 (K1 Media Raschig rings) during Stage II. The colour scale is shown on the right of the heatmap, which varies from low abundance (light yellow) to high abundance (deep red).

abundance increased during periods of starvation. This increase can be attributed to the consumption of the excess VFAs that were not metabolized during the normal operation period of the reactors. It is worth mentioning that in TBR-2 the dominance of bacteria over methanogens occurred from the beginning of Stage II, since it had a higher surplus of VFAs from Stage I compared to TBR-1, as illustrated in Fig. 8.

Delving deeper into the bacterial communities of the reactors, of great importance was the presence of *Coprothermobacter* genus. In particular, the relative abundance of *Coprothermobacter* genus in TBR-1 ranged from 1.1 % in the SP1, up to 26.6 % at the end of OP5, while in TBR-2, it had a high presence throughout the entire experimental period, reaching its highest percentage of 25.9 % in Period 1 (SP1). Similar studies observed that under alkaline conditions (pH 8.5–9.0) and at 55 °C, *Coprothermobacter* was the main functional bacteria [57]. Members of this genus are primarily known as thermophilic proteolytic bacteria that decompose proteins to produce hydrogen. Numerous research has also identified a synergistic relationship with hydrogenotrophic methanogens, in particular those belonging to the genus *Methanothermobacter* [58]. *Methanothermobacter* utilized the hydrogen produced by *Coprothermobacter* during decomposition to produce methane.

Moreover, the phylum *Firmicutes* presented a high abundance. Unfortunately, it was not possible to identify it to a higher taxonomic level. In particular, *Firmicutes_GGB26743* spp. and *Firmicutes_GGB27155* spp. showed the highest abundance, mainly in TBR-2. This phylum belongs to the homoacetogenic bacteria (homoacetogens) that can produce acetic acid from C1 compounds via the acetyl-CoA reduction pathway [59]. This assumption is supported in the present study, as during starvation periods there is an increase in VFA in TBR-2 that coincides with bacterial growth. During the last periods in both reactors the presence of the genus *Tepidiphilus* is noticeable, as according to the literature they are responsible for VFA consumption. The genus *Tepidiphilus* corresponds to the class of proteobacteria and is mainly thermophilic [64]. These microorganisms can use hydrogen or inorganic sulphur compounds as an electron source for chemotrophic growth and are capable of using acetate for heterotrophic growth [60]. *Tenericutes_GGB44214* spp. were not detected from the beginning of the experiment on TBR-1, in contrast to TBR-2 where they were present throughout the experiment, especially during normal operation of the reactors. This finding provides evidence that *Tenericutes* are bacteria, which can produce organic acids which occur during normal operation of the experiment [61].

4. Conclusions

The findings of this research highlight the efficacy of K1 Media Raschig rings over activated carbon pellets as a packing material in methane production, particularly at lower Gas Retention Times. This superiority is attributed to the formation of a well-structured biofilm and the predominant presence of the hydrogenotrophic thermophilic methanogen, *Methanothermobacter*, within the liquid media. Conversely, in on-demand biomethanation scenarios involving intermittent feeding of the reactors, activated carbon pellets demonstrated enhanced methane productivity from the first day of normal operation. This improved performance is linked to the establishment of a more appropriate environment, characterized by optimal pH and volatile fatty acids concentration, which favored the proliferation of the *Methanothermobacter* genus.

CRediT authorship contribution statement

Aikaterini Xirostylidou: Writing – original draft, Visualization, Investigation, Formal analysis, Data curation. **Maria Gaspari:** Writing – review & editing, Supervision, Methodology, Conceptualization. **Konstantinos N. Kontogiannopoulos:** Writing – review & editing, Visualization, Supervision, Software, Formal analysis. **Gabriele Ghiotto:** Software, Formal analysis, Writing – review and editing. **Laura Treu:** Writing – review & editing, Conceptualisation, Resources, Fundig acquisition. **Stefano Campanaro:** Writing – review & editing, Resources, Software. **Anastasios I. Zouboulis:** Writing – review & editing, Supervision, Resources. **Panagiotis G. Kougias:** Writing – review & editing, Supervision, Resources, Methodology, Funding acquisition, Conceptualization.

Declaration of competing interest

The authors declare that they have no known competing financial interests or personal relationships that could have appeared to influence the work reported in this paper.

Data availability

Data will be made available on request.

Acknowledgments

This project has received funding from the European Union's Horizon 2020 research and innovation program under grant agreement No. 101084405 (CRONUS). Views and opinions expressed are however those of the author(s) only and do not necessarily reflect those of the European Union or Horizon. Neither the European Union nor the granting authority can be held responsible for them.

References

[1] B.D. Jønson, L.O.L. Mortensen, J.E. Schmidt, M. Jeppesen, J.R. Bastidas-Oyanedel, Flexibility as the key to stability: optimization of temperature and gas feed during downtime towards effective integration of biomethanation in an intermittent energy system, Energies (Basel) 15 (2022), https://doi.org/10.3390/en15165827.
[2] M. Bailera, P. Lisbona, L.M. Romeo, S. Espatolero, Power to Gas projects review: Lab, pilot and demo plants for storing renewable energy and CO2, Renew. Sustain. Energy Rev. 69 (2017) 292–312, https://doi.org/10.1016/j.rser.2016.11.130.
[3] M. Götz, J. Lefebvre, F. Mörs, A. McDaniel Koch, F. Graf, S. Bajohr, R. Reimert, T. Kolb, Renewable Power-to-Gas: A technological and economic review, Renew. Energy 85 (2016) 1371–1390, https://doi.org/10.1016/j.renene.2015.07.066.
[4] C. Feickert Fenske, D. Strübing, K. Koch, Biological methanation in trickle bed reactors - a critical review, Bioresour Technol 385 (2023), https://doi.org/10.1016/j.biortech.2023.129383.
[5] R.K. Gopal, P.P. Raj, A. Dukare, R. Kumar, Metabolic Engineering of Methanogenic Archaea for Biomethane Production from Renewable Biomass, in: Biomethane, Apple Academic Press, 2022: pp. 43–60. doi: 10.1201/9781003277163-3.
[6] C. Feickert Fenske, F. Kirzeder, D. Strübing, K. Koch, Biogas upgrading in a pilot-scale trickle bed reactor – Long-term biological methanation under real application conditions, Bioresour. Technol. 376 (2023), https://doi.org/10.1016/j.biortech.2023.128868.
[7] B.D. Jønson, P. Tsapekos, M. Tahir Ashraf, M. Jeppesen, J. Ejbye Schmidt, J. R. Bastidas-Oyanedel, Pilot-scale study of biomethanation in biological trickle bed reactors converting impure CO2 from a Full-scale biogas plant, Bioresour. Technol. 365 (2022), https://doi.org/10.1016/j.biortech.2022.128160.
[8] W. Logroño, D. Popp, S. Kleinsteuber, H. Sträuber, H. Harms, M. Nikolausz, Microbial resource management for ex situ biomethanation of hydrogen at alkaline ph, Microorganisms 8 (2020), https://doi.org/10.3390/microorganisms8040614.
[9] Bioenergy Insight, Nature Energy and Andel inaugurate power-to-gas facility in Denmark, (2023). https://www.bioenergy-news.com/news/nature-energy-and-andel-inaugurate-power-to-gas-facility-in-denmark/(accessed March 14, 2024).
[10] Q. Sun, H. Li, J. Yan, L. Liu, Z. Yu, X. Yu, Selection of appropriate biogas upgrading technology-a review of biogas cleaning, upgrading and utilisation, Renew. Sustain. Energy Rev. 51 (2015) 521–532, https://doi.org/10.1016/j.rser.2015.06.029.
[11] H. Blanco, W. Nijs, J. Ruf, A. Faaij, Potential of Power-to-Methane in the EU energy transition to a low carbon system using cost optimization, Appl. Energy 232 (2018) 323–340, https://doi.org/10.1016/j.apenergy.2018.08.027.
[12] H. Porté, P.G. Kougias, N. Alfaro, L. Treu, S. Campanaro, I. Angelidaki, Process performance and microbial community structure in thermophilic trickling biofilter reactors for biogas upgrading, Sci. Total Environ. 655 (2019) 529–538, https://doi.org/10.1016/j.scitotenv.2018.11.289.
[13] M. Szuhaj, N. Ács, R. Tengölics, A. Bodor, G. Rákhely, K.L. Kovács, Z. Bagi, Conversion of H2 and CO2 to CH4 and acetate in fed-batch biogas reactors by mixed biogas community: A novel route for the power-to-gas concept, Biotechnol. Biofuels 9 (2016), https://doi.org/10.1186/s13068-016-0515-0.
[14] M.U. Monir, A. Yousuf, A.A. Aziz, Syngas fermentation to bioethanol, in: Lignocellulosic Biomass to Liquid Biofuels, Elsevier, 2019: pp. 195–216. doi: 10.1016/B978-0-12-815936-1.00006-X.
[15] P.T. Sekoai, A.A. Awosusi, K.O. Yoro, M. Singo, O. Oloye, A.O. Ayeni, M. Bodunrin, M.O. Daramola, Microbial cell immobilization in biohydrogen production: a short overview, Crit. Rev. Biotechnol. 38 (2018) 157–171, https://doi.org/10.1080/07388551.2017.1312274.
[16] L.L. Nesse, A.M. Osland, S.S. Mo, C. Sekse, J.S. Slettemeås, A.E.E. Bruvoll, A. M. Urdahl, L.K. Vestby, Biofilm forming properties of quinolone resistant Escherichia coli from the broiler production chain and their dynamics in mixed biofilms, BMC Microbiol. 20 (2020), https://doi.org/10.1186/s12866-020-01730-w.
[17] A. Chatzis, E. Orellana, M. Gaspari, K. Kontogiannopoulos, L. Treu, A. Zouboulis, P. G. Kougias, Comparative study on packing materials for improved biological methanation in trickle Bed reactors, Bioresour. Technol. 385 (2023), https://doi.org/10.1016/j.biortech.2023.129456.
[18] I. Angelidaki, L. Ellegaard, B.K. Ahring, Compact automated displacement gas metering system for measurement of low gas rates from laboratory fermentors, Biotechnol. Bioeng. 39 (1992) 351–353, https://doi.org/10.1002/bit.260390314.
[19] C. Anagnostopoulou, K.N. Kontogiannopoulos, M. Gaspari, M.S. Morlino, A. N. Assimopoulou, P.G. Kougias, Valorization of household food wastes to lactic acid production: A response surface methodology approach to optimize fermentation process, Chemosphere 296 (2022), https://doi.org/10.1016/j.chemosphere.2022.133871.
[20] A.M. Bolger, M. Lohse, B. Usadel, Trimmomatic: A flexible trimmer for Illumina sequence data, Bioinformatics 30 (2014) 2114–2120, https://doi.org/10.1093/bioinformatics/btu170.
[21] N. De Bernardini, A. Basile, G. Zampieri, A. Kovalovszki, B. De Diego Diaz, E. Offer, N. Wongfaed, I. Angelidaki, P.G. Kougias, S. Campanaro, L. Treu, Integrating metagenomic binning with flux balance analysis to unravel syntrophies in anaerobic CO2 methanation, Microbiome 10 (2022), https://doi.org/10.1186/s40168-022-01311-1.
[22] A. Blanco-Míguez, F. Beghini, F. Cumbo, L.J. McIver, K.N. Thompson, M. Zolfo, P. Manghi, L. Dubois, K.D. Huang, A.M. Thomas, W.A. Nickols, G. Piccinno, E. Piperni, M. Punčochář, M. Valles-Colomer, A. Tett, F. Giordano, R. Davies, J. Wolf, S.E. Berry, T.D. Spector, E.A. Franzosa, E. Pasolli, F. Asnicar, C. Huttenhower, N. Segata, Extending and improving metagenomic taxonomic profiling with uncharacterized species using MetaPhlAn 4, Nat. Biotechnol. (2023), https://doi.org/10.1038/s41587-023-01688-w.
[23] B. Langmead, S.L. Salzberg, Fast gapped-read alignment with Bowtie 2, Nat. Methods 9 (2012) 357–359, https://doi.org/10.1038/nmeth.1923.
[24] J.H. Merritt, D.E. Kadouri, G.A. O'Toole, Growing and analyzing static biofilms, Curr. Protoc. Microbiol. (2011), https://doi.org/10.1002/9780471729259.mc01b01s22.
[25] P. Ghofrani-Isfahani, P. Tsapekos, M. Peprah, P. Kougias, X. Zhu, A. Kovalovszki, A. Zervas, X. Zha, C.S. Jacobsen, I. Angelidaki, Ex-situ biogas upgrading in thermophilic up-flow reactors: The effect of different gas diffusers and gas retention times, Bioresour. Technol. 340 (2021), https://doi.org/10.1016/j.biortech.2021.125694.
[26] M. Namdarimonfared, H. Zilouei, H. Tondro, Biological hydrogen production from paper mill effluent via dark fermentation in a packed bed biofilm reactor, Fuel 338 (2023), https://doi.org/10.1016/j.fuel.2022.127231.
[27] L. Rachbauer, R. Beyer, G. Bochmann, W. Fuchs, Characteristics of adapted hydrogenotrophic community during biomethanation, Sci. Total Environ. 595 (2017) 912–919, https://doi.org/10.1016/j.scitotenv.2017.03.074.
[28] Z. Kusnere, K. Spalvins, D. Blumberga, I. Veidenbergs, Packing materials for biotrickling filters used in biogas upgrading – biomethanation, Agron. Res. 19 (2021) 819–833, https://doi.org/10.15159/AR.21.082.
[29] P.G. Kougias, P. Tsapekos, L. Treu, M. Kostoula, S. Campanaro, G. Lyberatos, I. Angelidaki, Biological CO2 fixation in up-flow reactors via exogenous H2 addition, J. Biotechnol. 319 (2020) 1–7, https://doi.org/10.1016/j.jbiotec.2020.05.012.
[30] P. Tsapekos, L. Treu, S. Campanaro, V.B. Centurion, X. Zhu, M. Peprah, Z. Zhang, P. G. Kougias, I. Angelidaki, Pilot-scale biomethanation in a trickle bed reactor: Process performance and microbiome functional reconstruction, Energy Convers Manag 244 (2021), https://doi.org/10.1016/j.enconman.2021.114491.
[31] P. Weiland, Biogas production: Current state and perspectives, Appl. Microbiol. Biotechnol. 85 (2010) 849–860, https://doi.org/10.1007/s00253-009-2246-7.
[32] R. Muñoz, L. Meier, I. Diaz, D. Jeison, A review on the state-of-the-art of physical/chemical and biological technologies for biogas upgrading, Rev. Environ. Sci. Biotechnol. 14 (2015) 727–759, https://doi.org/10.1007/s11157-015-9379-1.
[33] K. Baransi-Karkaby, M. Hassanin, S. Muhsein, N. Massalha, I. Sabbah, Innovative ex-situ biological biogas upgrading using immobilized biomethanation bioreactor (IBBR), Water Sci. Technol. 81 (2020) 1319–1328, https://doi.org/10.2166/wst.2020.234.
[34] N.M.C. Saady, Homoacetogenesis during hydrogen production by mixed cultures dark fermentation: Unresolved challenge, Int. J. Hydrogen Energy 38 (2013) 13172–13191, https://doi.org/10.1016/j.ijhydene.2013.07.122.
[35] S.T. Daglioglu, T.C. Ogut, G. Ozdemir, N. Azbar, Comparative Evaluation of Two Packing Materials (Glass Pipe and Ceramic Ball) for Hydrogenothrophic Biomethanation (BHM) of CO2, Waste Biomass Valoriz. 12 (2021) 3717–3726, https://doi.org/10.1007/s12649-020-01242-8.
[36] I. Casini, T. McCubbin, S. Esquivel-Elizondo, D. Evseeva, C. Fink, S. Beblawy, L. Aristilde, D.H. Huson, A. Dräger, E. Marcellin, L.T. Angenent, B. Molitor, An integrated systems-biology platform for power-to-gas technology 2, (n.d.). doi: 10.1101/2022.12.30.522236.
[37] A. Fontana, P.G. Kougias, L. Treu, A. Kovalovszki, G. Valle, F. Cappa, L. Morelli, I. Angelidaki, S. Campanaro, Microbial activity response to hydrogen injection in thermophilic anaerobic digesters revealed by genome-centric metatranscriptomics, Microbiome 6 (2018), https://doi.org/10.1186/s40168-018-0583-4.
[38] H. Jiang, F. Wu, Y. Wang, L. Feng, H. Zhou, Y. Li, Characteristics of in-situ hydrogen biomethanation at mesophilic and thermophilic temperatures, Bioresour. Technol. 337 (2021), https://doi.org/10.1016/j.biortech.2021.125455.
[39] S. Saha, B. Basak, J.H. Hwang, E.S. Salama, P.K. Chatterjee, B.H. Jeon, Microbial Symbiosis: A Network towards Biomethanation, Trends Microbiol. 28 (2020) 968–984, https://doi.org/10.1016/j.tim.2020.03.012.
[40] Y.W. Berkessa, B. Yan, T. Li, V. Jegatheesan, Y. Zhang, Treatment of anthraquinone dye textile wastewater using anaerobic dynamic membrane bioreactor: Performance and microbial dynamics, Chemosphere 238 (2020), https://doi.org/10.1016/j.chemosphere.2019.124539.
[41] M.S.M. Jetten, A.J.M. Stams, A.J.B. Zehnder, Methanogenesis from acetate: a comparison of the acetate metabolism in Methanothrix soehngenii and Methanosarcina spp, FEMS Microbiol. Lett. 88 (1992) 181–198, https://doi.org/10.1111/j.1574-6968.1992.tb04987.x.
[42] W. Logroño, D. Popp, M. Nikolausz, P. Kluge, H. Harms, S. Kleinsteuber, Microbial Communities in Flexible Biomethanation of Hydrogen Are Functionally Resilient Upon Starvation, Front. Microbiol. 12 (2021), https://doi.org/10.3389/fmicb.2021.619632.

[43] H. Khesali Aghtaei, S. Püttker, I. Maus, R. Heyer, L. Huang, A. Sczyrba, U. Reichl, D. Benndorf, Adaptation of a microbial community to demand-oriented biological methanation, Biotechnol. Biofuels Bioprod. 15 (2022), https://doi.org/10.1186/s13068-022-02207-w.
[44] M.B. Jensen, S. Poulsen, B. Jensen, A. Feilberg, M.V.W. Kofoed, Selecting carrier material for efficient biomethanation of industrial biogas-CO2 in a trickle-bed reactor, J. CO2 Util. 51 (2021), https://doi.org/10.1016/j.jcou.2021.101611.
[45] C. Barca, A. Soric, D. Ranava, M.T. Giudici-Orticoni, J.H. Ferrasse, Anaerobic biofilm reactors for dark fermentative hydrogen production from wastewater: A review, Bioresour. Technol. 185 (2015) 386–398, https://doi.org/10.1016/j.biortech.2015.02.063.
[46] D. Strübing, A.B. Moeller, B. Mößnang, M. Lebuhn, J.E. Drewes, K. Koch, Load change capability of an anaerobic thermophilic trickle bed reactor for dynamic H2/CO2 biomethanation, Bioresour. Technol. 289 (2019), https://doi.org/10.1016/j.biortech.2019.121735.
[47] L. Braga Nan, E. Trably, G. Santa-Catalina, N. Bernet, J.P. Delgenes, R. Escudie, Microbial community redundance in biomethanation systems lead to faster recovery of methane production rates after starvation, Sci. Total Environ. 804 (2022), https://doi.org/10.1016/j.scitotenv.2021.150073.
[48] P.G. Kougias, I. Angelidaki, Biogas and its opportunities—A review, Front. Environ. Sci. Eng. 12 (2018), https://doi.org/10.1007/s11783-018-1037-8.
[49] M.T. Ashraf, M.U. Sieborg, L. Yde, C. Rhee, S.G. Shin, J.M. Triolo, Biomethanation in a thermophilic biotrickling filter — pH control and lessons from long-term operation, Bioresour Technol. Rep. 11 (2020), https://doi.org/10.1016/j.biteb.2020.100525.
[50] T.L. Dupnock, M.A. Deshusses, High-Performance Biogas Upgrading Using a Biotrickling Filter and Hydrogenotrophic Methanogens, Appl. Biochem. Biotechnol. 183 (2017) 488–502, https://doi.org/10.1007/s12010-017-2569-2.
[51] R.M. Wormald, S.P. Rout, W. Mayes, H. Gomes, P.N. Humphreys, Hydrogenotrophic Methanogenesis Under Alkaline Conditions, Front. Microbiol. 11 (2020), https://doi.org/10.3389/fmicb.2020.614227.
[52] M.U. Sieborg, B.D. Jønson, M.T. Ashraf, L. Yde, J.M. Triolo, Biomethanation in a thermophilic biotrickling filter using cattle manure as nutrient media, Bioresour. Technol. Rep. 9 (2020), https://doi.org/10.1016/j.biteb.2020.100391.
[53] S. Savvas, J. Donnelly, T. Patterson, Z.S. Chong, S.R. Esteves, Methanogenic capacity and robustness of hydrogenotrophic cultures based on closed nutrient recycling via microbial catabolism: Impact of temperature and microbial attachment, Bioresour. Technol. 257 (2018) 164–171, https://doi.org/10.1016/j.biortech.2018.02.109.
[54] D. Strübing, A.B. Moeller, B. Mößnang, M. Lebuhn, J.E. Drewes, K. Koch, Anaerobic thermophilic trickle bed reactor as a promising technology for flexible and demand-oriented H2/CO2 biomethanation, Appl. Energy 232 (2018) 543–554, https://doi.org/10.1016/j.apenergy.2018.09.225.
[55] A.D. Dorado, F.J. Lafuente, D. Gabriel, X. Gamisans, A comparative study based on physical characteristics of suitable packing materials in biofiltration, Environ. Technol. 31 (2010) 193–204, https://doi.org/10.1080/09593330903426687.
[56] M. Palù, M. Peprah, P. Tsapekos, P. Kougias, S. Campanaro, I. Angelidaki, L. Treu, In-situ biogas upgrading assisted by bioaugmentation with hydrogenotrophic methanogens during mesophilic and thermophilic co-digestion, Bioresour. Technol. 348 (2022), https://doi.org/10.1016/j.biortech.2022.126754.
[57] L. Chen, S. Du, L. Xie, Effects of pH on ex-situ biomethanation with hydrogenotrophic methanogens under thermophilic and extreme-thermophilic conditions, J. Biosci. Bioeng. 131 (2021) 168–175, https://doi.org/10.1016/j.jbiosc.2020.09.018.
[58] M.C. Gagliano, C.M. Braguglia, A. Gianico, G. Mininni, K. Nakamura, S. Rossetti, Thermophilic anaerobic digestion of thermal pretreated sludge: Role of microbial community structure and correlation with process performances, Water Res. 68 (2015) 498–509, https://doi.org/10.1016/j.watres.2014.10.031.
[59] K. Igarashi, S. Kato, Reductive Transformation of Fe(III) (oxyhydr)Oxides by Mesophilic Homoacetogens in the Genus Sporomusa, Front. Microbiol. 12 (2021), https://doi.org/10.3389/fmicb.2021.600808.
[60] C.M. Manaia, B. Nogales, O.C. Nunes, Tepidiphilus margaritifer gen. nov., sp. nov., isolated from a thermophilic aerobic digester, Int. J. Syst. Evol. Microbiol. 53 (2003) 1405–1410, https://doi.org/10.1099/ijs.0.02538-0.
[61] G. Zhu, Q. Feng, K. Wang, Y.C. Song, Y. Zhou, Q. Zhou, Investigating the performance of different applied voltages on lignite biomethanation in microbial electrolytic cell coupled anaerobic digestion, Int. J. Hydrogen Energy (2023), https://doi.org/10.1016/j.ijhydene.2023.09.007.
[62] G. Ghiotto, G. Zampieri, S. Campanaro, L. Treu, Strain-resolved metagenomics approaches applied to biogas upgrading, Environ Res 240 (2024), https://doi.org/10.1016/j.envres.2023.117414.
[63] G. Ghiotto, N. De Bernardini, G. Giangeri, P. Tsapekos, M. Gaspari, P.G. Kougias, S. Campanaro, I. Angelidaki, L. Treu, 2024. From microbial heterogeneity to evolutionary insights: A strain-resolved metagenomic study of H2S-induced changes in anaerobic biofilms, J Chem Eng 485 (2024) https://doi.org/10.1016/j.cej.2024.149824.
[64] V.B. Centurion, A. Rossi, E. Orellana, G. Ghiotto, B. Kakuk, M.S. Morlino, A. Basile, G. Zampieri, L. Treu, S. Campanaro, A unified compendium of prokaryotic and viral genomes from over 300 anaerobic digestion microbiomes, Environ Microbiome 19 (2024), https://doi.org/10.1186/s40793-023-00545-2.
[65] F. Ebrahimian, N. De Bernardini, P. Tsapekos, L. Treu, S. Campanaro, K. Karimi, I. Angelidaki, Effect of pressure on biomethanation process and spatial stratification of microbial communities in trickle bed reactors under decreasing gas retention time, Bioresour Technol (2022).